Investigation of Thermal Behavior of an Oil Directed Cooled Transformer Winding

S. Tenbohlen, *Senior Member, IEEE,* N. Schmidt, C. Breuer, S. Khandan, R. Lebreton

***Abstract*—In this contribution the oil speed in horizontal channels of an OD (oil-directed) cooled winding is investigated by experimental and numerical methods. The presented winding model offers insight into the horizontal cooling channels perpendicular to the main oil flow direction. To visualize the oil flow, tracing particles were added to the cooling oil and illuminated by high power LEDs. The particle velocities were then determined by taking photographs with a defined exposure time. The design of the sophisticated winding model is described in the contribution. In addition to the experimental results, this contribution presents a comparison with respective numerical results from 2D and 3D CFD calculations. Finally, numerical results from the winding model concerning the oil flow distribution inside the winding at various operating conditions are presented. The investigation indicated a strong non-uniform oil flow distribution on the horizontal channels. The presented results give a deep insight into the oil flow and temperature behavior of windings enabling the designer to optimize the cooling of power transformer windings.**

***Keywords*—Power Transformer, Oil-directed Cooling, Optical Investigation, Thermal Modelling, Computational Fluid Dynamics, Oil Flow Rate**.

I. Introduction[1]

Power transformers are key components applied in transmission and distribution systems. Their power rating and life cycle characteristics are strongly dependent on thermal aspects. The higher the evolving temperature levels at a given loading rate are settling, the faster the insulation materials will age at that loading rate. Therefore, a profound knowledge about the temperature distribution inside a transformer is crucial for an appropriate assessment of the component's power rating and for that reason offers the opportunity to cut costs in the production process. In the past, and still today to some extent, analytical and empirical methods have been used to predict the temperature distribution in the transformer components and to determine the hot-spot value. A Literature survey based on IEEE Transactions in [1] revealed the continued interest in the application of advanced techniques for transformers design optimization. For the investigation of the temperature distribution within the windings of an OD cooled transformer, different approaches can be pursued [2].

The importance of winding hotspot determination is reflected in published efforts to predict the hot-spot temperature in the windings. The thermal-hydraulic networks (THN) can be used for describing the entire oil circuit in order to investigate natural circulations [3-5]. However, it has been shown in the literature that comparing with the THN, the CFD method provides better accuracy in prediction of the temperature distributions and fluid behaviors [6-8].

Thermal modeling offers a detailed view of temperature distribution over the whole winding and temperature values at the characteristic points. The originally developed algorithm thermal modeling network for temperature calculations is based on characteristic temperatures.

An efficient thermal design offers the opportunity to significantly reduce costs in the production process and to improve the thermal performance [9]. Due to the numerical simulations with CFD techniques, a better comprehension of the cooling mechanism of core type transformers has developed to high levels.

In recent years, most of the numerical models are considered in 2D approach. El Wakil et al. [10] have performed a 2D simulation of a step-down 3-phase power transformer that included the core, primary and secondary windings using a commercial finite volume code. Skillen et al. have [11] investigated on a 2D axisymmetric model the local hot-spot in detail within the low-voltage winding and predicted with CFD simulations the hot streak locations. Mufuta et al. [12] have presented 2D results of the flow pattern as a function of the Reynolds and Grashof numbers as well as of geometric parameters. Gastelurrutia et al. [13] have performed the CFD solutions for an ONAN distribution layer-type transformer. Their model simulated the natural convection behavior within the power transformers and displayed the oil flow behavior inside distribution layer-type transformers. A 2D CFD model is used also to recognize the significant effects of buoyancy term and hot oil streak formations, the latter of which could more or less worsen downstream oil temperatures [14]. Dimensional analyses are conducted in 2D OD cooled winding model to identify the independent dimensionless variables that effect pressure drops in the windings [15]. Torriano et al. [16] have focused on the parameters affecting on the temperature distributions and fluid flow in the winding.

Besides the 2D approach for simulating thermal behaviors of windings, 3D approach is also employed to determine the temperature distributions and fluid flow in recent CFD

S. Tenbohlen, N. Schmidt and S. Khandan are with the Institute of Power Transmission and High Voltage Technology (IEH), University of Stuttgart, Stuttgart 70569, Germany. (e-mails: stefan.tenbohlen@ieh.uni-stuttgart.de, nicolas.schmidt@ieh.uni-stuttgart.de, saeed.khandan@ieh.uni-stuttgart.de).

C. Breuer is with GE Grid Solution in Moenchengladbach, R&D Engineer Power transformers, (e-mail: christian.breuer@ge.com).

R. Lebreton is with GE Grid Solution, R&D Engineer Power transformers, GE Grid Solutions in Paris. (e-mail: raphael.lebreton@ge.com).

calculations. A low-voltage winding has been simulated and the results show that the performances of the 3D numerical computations are significantly better than that of the 2D models [17]. Smolka et al. [18] have presented full geometry CFD analyses coupled to electromagnetic simulations to examine the specific power losses within the coil and core of a dry-type transformer. Campelo et al. [19] have predicted for the OD cooling modes with high flow velocities, a stagnant flow or even reverse flow can be observed in the first horizontal channels of the pass. A comprehensive review of the thermal modeling in power transformers, state of the art as well as a proper literature review has become available in [9].

In this contribution, the oil speed in horizontal ducts of an OD cooled winding is investigated by experimental and numerical methods.

Representatively for often used winding types, a so-called "zigzag" arrangement of a disc-type winding was investigated. In such a case, winding discs are layered above each other, while so-called spacers keep the axial distance between the discs and determine the height of the horizontal ducts for the oil. The sticks ensure the proper fixation of the spacers and keep the radial distance between the discs and the outer cover. The vertical ducts are formed by the space between discs and outer cover. The oil is led from the bottom into the vertical ducts and flows from there upwards, while it distributes into the particular horizontal ducts. To ensure a proper distribution of the oil to the horizontal ducts, which should be as equal as possible, the vertical duct is intermitted alternating between the inner and the outer duct after a specified number of discs by so-called washers. This leads to an oil flow in a "zigzag" manner.

In order to confirm the suitability of a numerical 3D winding model to predict the realities in transformer windings accurately, a comparison between experimentally determined oil flow velocities with corresponding numerical data is presented in the paper.

II. Development of an Experimental Model for a Disc Winding

The design of disc type transformer windings shows a strong symmetry in the circumferential direction and can be subdivided into symmetrical sections. Fig. 1 shows a three dimensional view on a disc type winding with four turns per disc. The given enlargement shows the horizontal cooling channels are created by the opening between two consecutive spacers and discs. The vertical cooling channels are bounded by the cardboard cylinders and by the sticks aligning the spacers. Consequently, the entire winding geometry can be subdivided into symmetrical sections. For reasons of an improved visibility concerning the cooling system inside the winding, the outer cardboard cylinder is displayed in a partly transparent color.

The investigated operating conditions are defined by the temperature of the oil entering the model, the oil flow rate passing the winding model and the losses supplied to each conductor model. However, since the latter two properties refer strictly to a single symmetrical section, they are not easy to put into perspective of common transformer design rules. Since common transformer design rules usually refer to entire windings, the properties given in this contribution, to reference investigated operating conditions, are transferred accordingly. For example, instead of specifying the heating power per conductor model representing a section of 8° in the circumferential direction of on entire winding turn, the corresponding losses per complete winding turn are referenced. Analogous considerations are applied for the oil flow rate. For that reason, the actually applied heating power per conductor model and the oil flow rates passing the winding models are 8°/360° = 1/45 times the referenced values pointed out in the figure captions.

A top view of a symmetric section of this chosen winding design including all relevant geometric details to assess this design is shown in Fig. 2. Since the exact reproduction of this geometry in Fig. 2a imposes enormous challenges for the connected manufacturing processes, the respective design of the experimental model was modified. For that purpose, the curvature of the conductors in circumferential direction is neglected, as displayed in Fig. 2b. To eliminate the detrimental influences of neglecting the curvature in 8°, all the dimensions are selected according to the symmetrical section.

The paper wrapping typically applied around conductors in transformer windings for purposes of an electrical insulation is substituted by solid blocks of plastic (Polyvinylidenefluoride) located only in between the conductors of a disc. Prior experimental investigations showed a great sensitivity to the evolving temperature levels on the exact thickness of the applied paper wrapping. Unfortunately, this property, especially with regard to the comparably short experimental conductor models, is difficult to keep within small tolerances. To eliminate respective detrimental influences but still allow a realistic thermal decoupling of the conductor models in one disc, the paper is substituted, as illustrated in detail in Fig. 2c. In this contribution the inlet temperature is set to ϑ_{in} = 80°C while the oil flow rates are set to $\dot{m}_{oil}$ = 3 kg/s, $\dot{m}_{oil}$ = 9 kg/s and $\dot{m}_{oil}$ = 18.0 kg/s. The losses per winding turn are kept at $P_{losses,\,i}$ = 360 W/turn.

To provide the heating power normally dissipated in the winding turns of a power transformer during operation, heating cartridges are injected into each conductor model through a borehole. An accurate measurement of the conductors' temperature is accomplished with temperature sensors located inside each conductor. The cooling system of OD cooled disc windings is usually subdivided into so-called passes in the axial direction.

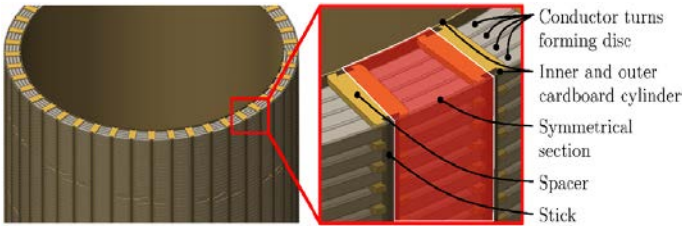

Fig. 1. Basic winding design and alignment of spacers creating symmetrical sections with periodic cooling channel system [20].

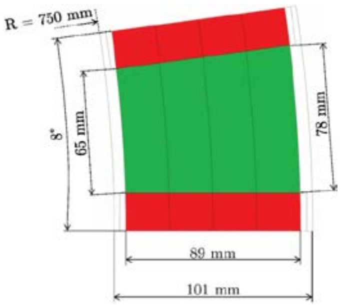

a) Top view on winding segment

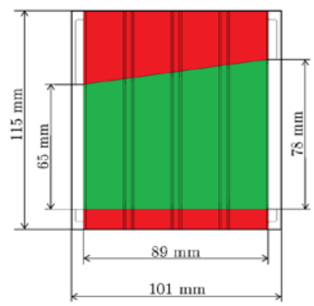

b) Cross section of winding model

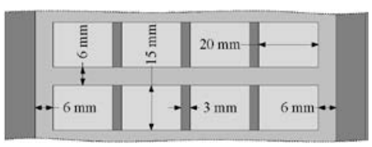

c) Cross section of winding model with given channel dimensions and insulation thickness applied between conductors resembling thermal impact of electrical insulation.

Fig. 2. Design characteristics of the modelled winding, geometry and the winding model [20].

By periodical placement of washers inside the vertical channels alternating between the inner and outer winding diameter, two different types of passes result. Therefore, the experimental winding model must consist of at least two consecutive passes. In addition, representative entering and exiting conditions are required before and after the investigated passes. This ensures thermal and hydraulic conditions that are representative for every pass throughout the complete cooling system of the modelled winding. Fig. 3a shows the chosen winding model layout in a schematic view as well as a clear reference for the pass, disc and conductor numbering upon which the presented post analysis relies. Next to a representative winding design, also the operating conditions of the modelled winding are chosen accordingly with respect to the winding type and dimensions. Fig. 3b contains a photo of the experimental winding model during operation.

Fig. 4 depicts schematically the designed experimental setup in which the flow meter, the flow heater, the gear pump and a control unit for supplying power to each heating cartridges are employed for obtaining the boundary conditions precisely. It allows an accurate control over the mass flow rate $\dot{m}_{\mathrm{oil}}$, the oil temperature at the model inlet ϑ_{in} and the heating power of each conductor $P_{\mathrm{losses},\,i}$. While the oil inlet temperature is set via a controlled flow heater, the initially provided oil flow rate from a gear pump is limited to a defined value by a controlled valve processing data from a flowmeter. Furthermore, two temperature sensors are employed at inlet of the winding in order to guarantee that there is no deviation between the oil temperature provided by the flow heater sensor and that entering the winding model.

To minimize the heat leakage from the winding model to its surroundings, the entire model is submerged in an open experimental tank filled with oil of the same temperature as provided by the flow heater. Due to the chosen laboratory setup, a total measuring tolerance concerning the temperatures of approximately 0.5 K is achieved. Consequently, temperature gradients can be determined with an accuracy of around 1 K.

The occurring deviations concerning the mass flow measurement and heating power control are below 1 %. Because oil is a transparent liquid, the investigation of the oil flow requires additional measures. For that purpose, tracing particles were added to the oil of the experimental setup.

These particles were chosen according to the material properties of the mineral oil and the application conditions of the investigation. To make the particles visible, a strong source of light has to be applied. High power LEDs were mounted directly in front of the horizontal channels in experimental setup, as indicated in Fig. 5.

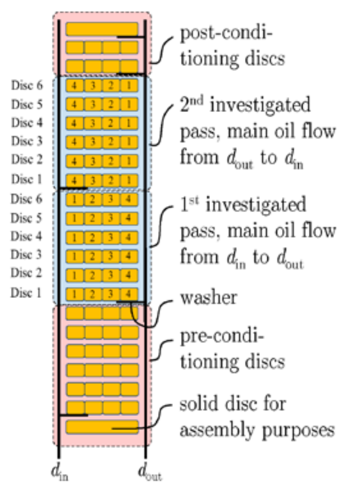

a) Schematic layout of experimental winding model.

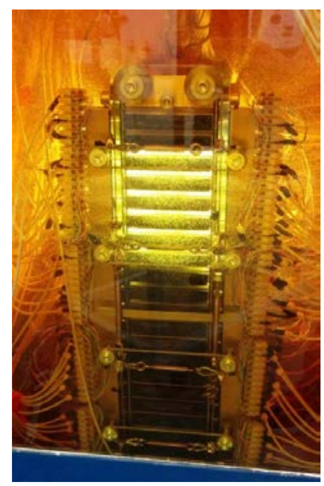

b) Experimental winding model in tank during operation.

Fig. 3. Components of a conductor model for the experimental winding model [20].

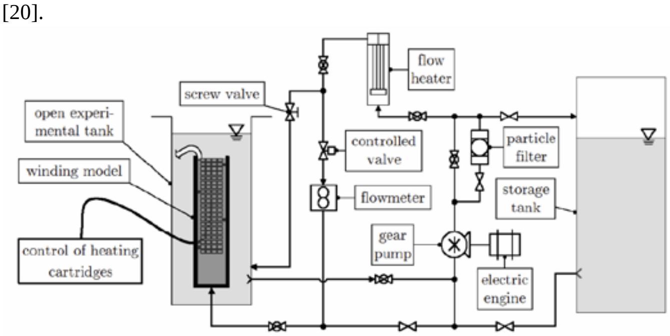

Fig. 4. Piping and instrumentation diagram of the laboratory setup designed to create strictly controlled boundary conditions inside the winding model [20].

A digital camera was then mounted in a defined alignment of the horizontal channels and focused on the investigated area in the middle of the horizontal channels. Due to the chosen optical equipment and the connected setup, the depth of field defining the investigated areas in the *z*-Dimension shown in Fig. 5 are limited to approx. 6 mm. The particle velocities within the investigated area were then determined by taking photographs applying a defined exposure time. Firstly, a reference picture of a glass spacer is taken to create common scale for one measurement set, then the camera is aligned in front of the first channel of pass and the optical focus is set between the solid spacer and the glass spacer. Depending on the oil flow velocity in the respective channel, an appropriate setup for the LED power level and the chosen shutter are determined. It should be noted that for each pass during the measurement, distance between the camera and the model are kept constant. After measuring the particle track lengths in the taken pictures, the particle velocities can be calculated with the relation as follows:

Local velocity of particle v_i *= (Length of path line of particle i* l_i*) / (Selected shutter speed* Δt*)* (1)

As demonstrated in Fig. 6, the analysed area is also limited in the *y*-Dimension and in the *x*-Dimension to the exit location of the oil inside the horizontal channels.

For that reason, only particles inside a volume of approximately 20 mm × 2 mm × 6 mm ($x \times y \times z$) were analysed within each channel. This restriction is necessary since the oil flow velocities are not expected to be homogeneously distributed. Consequently, the investigated area should be as small as possible. However, since the velocities might also fluctuate over time due to effects of turbulences, a certain number of particle tracks need to be considered for each investigated area. Since the number of particles captured on photograph inside a certain area is directly dependent on the size of the investigated area, a compromise between restricting the investigated area and the resulting number of available particle tracks recorded for post analysis had to be made.

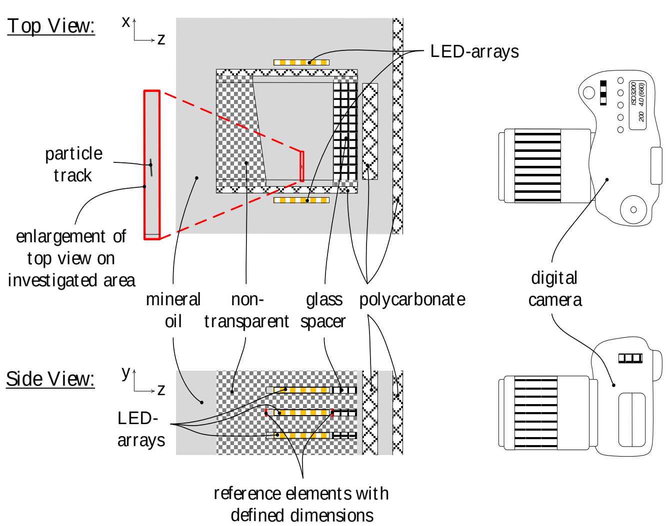

Fig. 5. Experimental setup of the optical analysis [23].

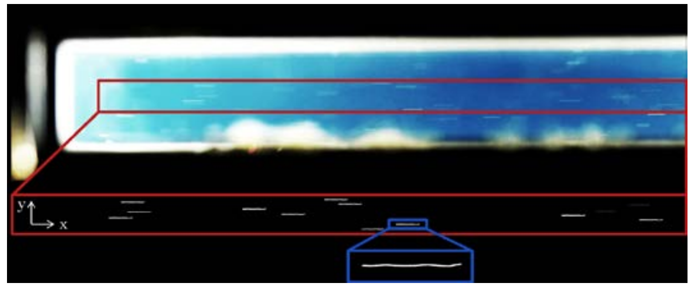

Fig. 6. Example of a photograph of particle tracks with contrast enhancement and enlargement of the investigated area in the taken pictures and further enlargement of one particle track [23].

III. CFD Model

The development of numerical winding models suitable for CFD analysis first of all comprises the definition and creation of respective modelling domains [3]. In case of a 3D winding model, the common design of disc windings allows a significant reduction of the winding geometry in circumferential direction, as carried out for the experimental winding model described above. In addition, the symmetric alignment of the spacers inside a symmetrical winding section, offers potential for further reduction by application of symmetric boundary conditions, as indicated in Fig. 7.

The chosen modelling domain of the 2D winding model, allowing a significant reduction of the connected computational efforts, requires further explanation. Since ANSYS CFX does not feature a dedicated 2D solver, even the analysed 2D geometry must consist of 3D finite volumes. However, since only one layer of 3D cells is necessary, the detrimental consequences resulting from this requirement are negligible. On the contrary, modelling the winding geometry with a 2D domain can even take advantage of this restriction by creating a 2D modelling domain featuring a non-uniform cell depth in third dimension [21]. Therefore, the widening of the horizontal cooling channels from inner to outer winding diameter, as displayed in Fig. 7, can also be acknowledged in the 2D winding model. The chosen 2D cell depths represent a defined fraction of the existing opening widths of the horizontal cooling channels.

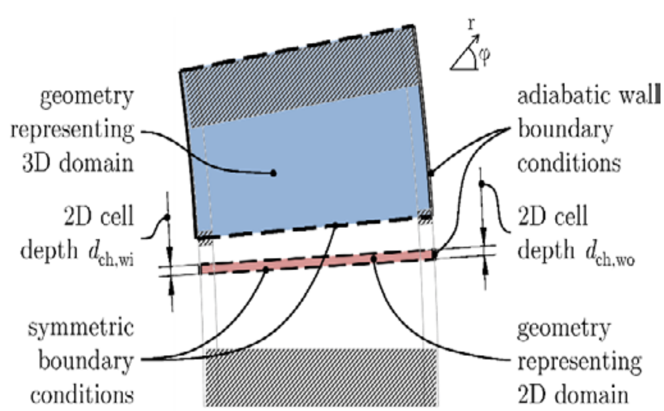

Fig. 7. Modelling domains of the numerical winding models created for CFD-analysis [20].

Nevertheless, due to the restriction of the 2D approach in CFX, it does not account for influence of side surface of spacers. Since the spacers are covering a certain area of the heat-transferring surface on the conductors, the numerical model assumes no heat transfer at these areas.

After the described choice of the respective modelling domains, the creation of the CFD winding models comprises the discretization process including the determination of an appropriate meshing density. Next to the global mesh size, special attention has to be paid towards the discretization of the boundary layers. The total number of hexahedral meshes employed for discretization of the 2D and 3D domains are approx. 7×10^6 cells and approx. 200×10^6, respectively. Due to the connected computational efforts, only the analysis of the 2D domain should be considered for state of the art desktop workstations. For a more efficient analysis following the described approach, high performance computing centers become advisable.

Table 1 gives three different operation points corresponding to the mass flow rates equal to $\dot{m}_{oil}$ = 3 kg/s, $\dot{m}_{oil}$ = 9 kg/s and $\dot{m}_{oil}$ = 18.0 kg/s with reference inlet temperature of 80°C. For the determination of the Reynolds numbers, the reference flow rate is calculated at the smallest hydraulic diameter through which the entire oil should pass, inside the vertical channel on the inner winding diameter side located across the oil washer. Table 1 gives the calculated Reynolds numbers for different operation conditions.

TABLE 1
INVESTIGATED OPERATING CONDITIONS AND RESPECTIVE REYNOLDS.

Operating points	Mass flow rate [kg/s]	inlet temperature [°C]	Reynolds numbers [1]
1	3	80	667
2	9	80	2000
3	18	80	4000

Operating point 1 indicates the analysis of the heat transfer at a low Reynolds number. The behavior of the fluid flow in the low Reynolds number is laminar, whereas operating points 2 and 3 indicate the analysis at higher Reynolds numbers, where the application of turbulence model is required to achieve accurate results with CFD simulations since the laminar character of the oil is affected by high oil flow rates with high inlet temperature. Turbulent numerical models are defined by an identical solver setup, which applies the SST (Shear Stress Transport) turbulence model [22] with its transitioning onset model at different operating conditions.

IV. RESULTS OF THE OPTICAL ANALYSIS REGARDING OIL VELOCITY

After determining the particle velocities in a certain channel at specific operating condition, the gathered data is further post-processed. To illustrate this process, Fig. 8 shows the distribution of measured particle velocities in channel 6 at the defined operating conditions in the context of an idealized Gaussian distribution function. Since this distribution function appears suitable for the collected measurement data, it is applied for the post-processing of the experimental results. Fig. 9 gives the results at specified operating conditions in pass 1. Next to the averaged, minimum and maximum values the displayed boxes illustrate the amount of scattering experienced during post-processing the measurements. For that purpose, the boxes enclose the range of measured values comprising 80% of all conducted measurements according to a Gaussian distribution. It can be noted, that especially the first and last channel show a wider distributed velocity distribution within the investigated area. While the experimental determination of the oil flow distribution is extensive, the corresponding numerical data can be extracted from the CFD result files. Fig. 10 shows the comparison of the experimental results and the 2D and 3D numerical post analyses at various operating conditions in pass 1 of the winding model. For comparing both approaches, measured data are compared with both numerical models.

The respective numerical data at middle cross-section in the 3D winding model of horizontal channels are given as well. Especially in the first channels the analysed location is of great influence on the determined velocity. This can be attributed to separation eddies at the duct entrance (see Fig. 12).

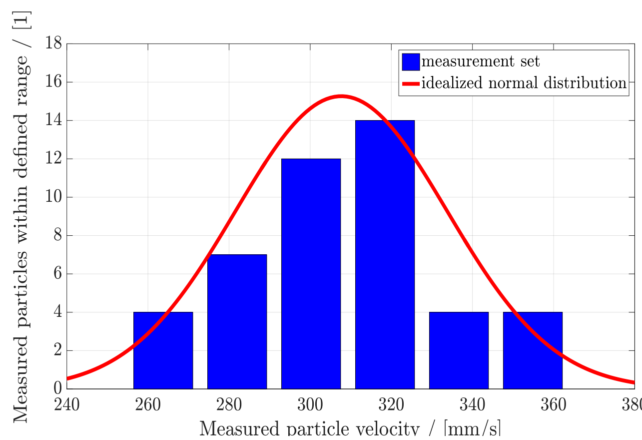

Fig. 8. Distribution of measured velocities in channel number 6 of pass 1 at $\dot{m}_{oil}$ = 9.0 kg/s, ϑ_{in} = 40°C and $P_{losses,\ i}$ = 360 W/turn with illustration of an idealized distribution according to a Gaussian distribution function [23].

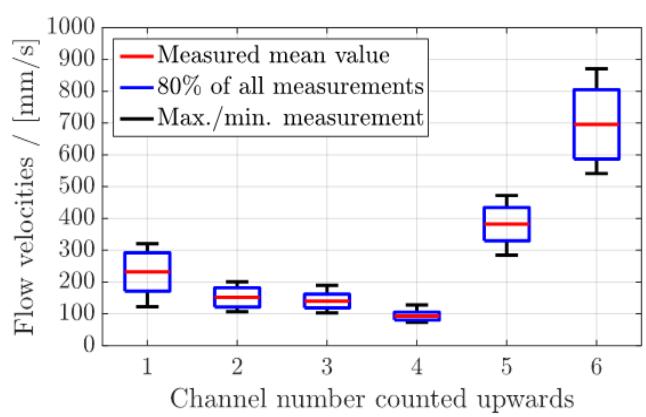

Fig. 9. Distribution of the determined oil flow velocities in pass 1 at $\dot{m}_{oil}$ = 18.0 kg/s, ϑ_{in} = 80°C and $P_{losses,\ i}$ = 360 W/turn [23].

This article has been accepted for publication in a future issue of this journal, but has not been fully edited. Content may change prior to final publication. Citation information: DOI 10.1109/TPWRD.2017.2711786, IEEE Transactions on Power Delivery

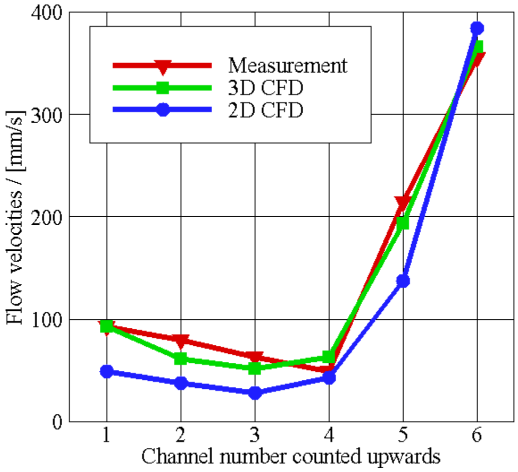

Fig. 10. Comparison of measured with 2D and 3D numerical calculated mid channel velocities in pass 1, $\dot{m}_{oil}$ = 9.0 kg/s, ϑin = 80°C, $P_{losses,\,i}$ = 360 W/turn.

The measured mean values agree impressively well with the numerical results in middle position at all operating conditions. Since the thermal investigation shows great agreement between experimental and numerical results, the respective results for the oil flow velocities are also in good agreement. The numerical results for the oil flow distribution are consequently also assumed to be valid. The velocity is proportional to the oil mass in the channels. By calculation of the average of the velocities in each channel, the shares of oil flow on the horizontal channels are determined at three different flow rates as shown in Fig. 11.

The high velocity of the oil after passing the washer (see also Fig. 13a) is the reason for the formation of the separation eddies. The oil flow in the lower ducts is becoming very small and can even turn to backflow. In order to investigate the reason for the uneven fluid flow distribution in Fig. 11, Fig. 12 shows the streamlines of the oil flow for a flow rate of 9 kg/s. The results of the CFD simulation indicate that the flow distributions on the horizontal oil channels are not equally. For

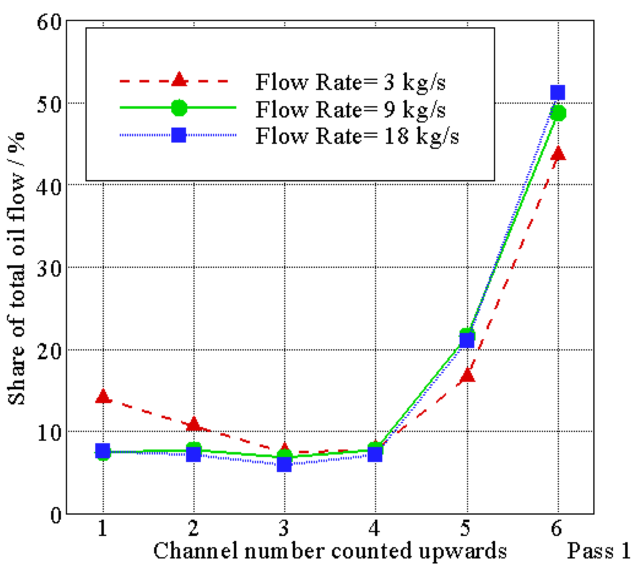

Fig. 11. Oil flow distribution onto horizontal channels in pass 1, ϑ_{in} = 80°C, $P_{losses,\,i}$ = 360 W/turn.

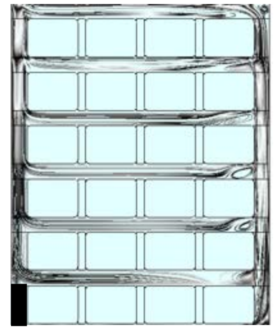

Fig. 12. Streamlines at a flow rate of $\dot{m}_{oil}$ = 9.0 kg/s

low flow rate of 3 kg/s, the maximum velocity occurs in the lower part of the pass, whereas for high winding flow rates shifts to the upper region of the passes. It gets obvious that separation eddies are blocking the entry of the horizontal channels.

V. Location of Hot Spot

One central objective of this contribution is the assessment of the pursued numerical modelling approaches for transformer windings. Since 3D winding models require significantly higher computational efforts in comparison to the 2D approach, it is of keen interest if those additional efforts are justified. To start the respective comparison between the 2D and 3D winding model, Fig. 13 shows the numerical results for the oil flow distribution inside the winding models for an oil flow rate of 18.0 kg/s qualitatively.

Although no quantitative comparison of the oil amount passing the different horizontal channels is carried out, the chosen visualization already gives a clear insight into the respective differences resulting from the chosen modelling approach. While the 2D winding model by definition suggests a homogeneous oil flow distribution in the circumferential direction, the 3D results clearly contradict this assessment. Especially the visible oil flow in the vertical channels of the 3D winding model displays a strong heterogeneous character.

However, because the oil flow distribution is only of secondary interest in comparison to the temperature distribution, Fig. 14 gives the results of the respective temperatures within the investigated winding geometry for pass1 of the 3D winding model for an oil flow rate of 9.0 kg/s. In the investigated arrangement the location of the hot spot is in the middle two discs (3 and 4), which is in contradiction with the common thinking that the hot spot can be found on top of the winding. The reason for this behavior is the non-uniform distribution of the oil flow as seen in Fig. 11. The oil velocity in the two last horizontal channels is much higher as in the four lower channels which results in a better cooling of these discs. Even the turns within one disc do not have the same temperature due to the thermal resistance of the insulation material between the turns. To better quantify the deviations connected to the numerical modelling setup, Fig. 15 presents the results for the temperature gradients between oil and conductors at all investigated operating conditions in the second pass of the winding model.

This article has been accepted for publication in a future issue of this journal, but has not been fully edited. Content may change prior to final publication. Citation information: DOI 10.1109/TPWRD.2017.2711786, IEEE Transactions on Power Delivery

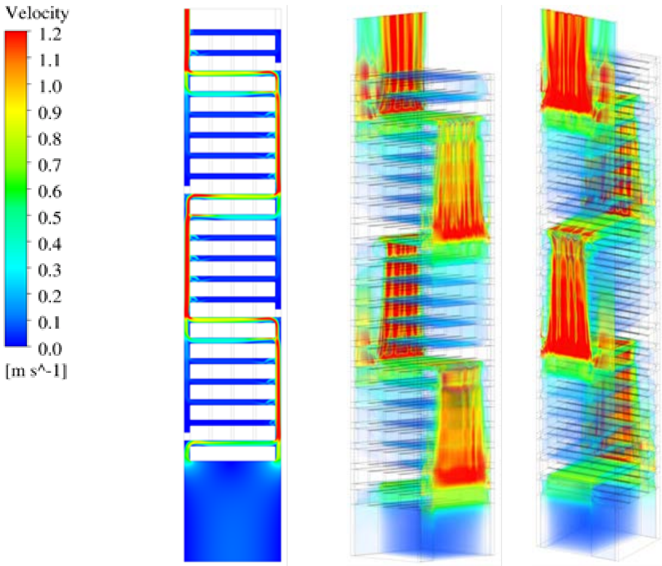

a) 2D model (d_{in} on left side)

b) 3D model (d_{out} in front) inner view

c) 3D model (d_{in} in front) outer view

Fig. 13. Comparison of the oil flow velocities within the 2D and 3D CFD winding model at $\dot{m}_{oil}$ = 18.0 kg/s, ϑ_{in} = 80°C and P_{losses} = 360 W/turn [20].

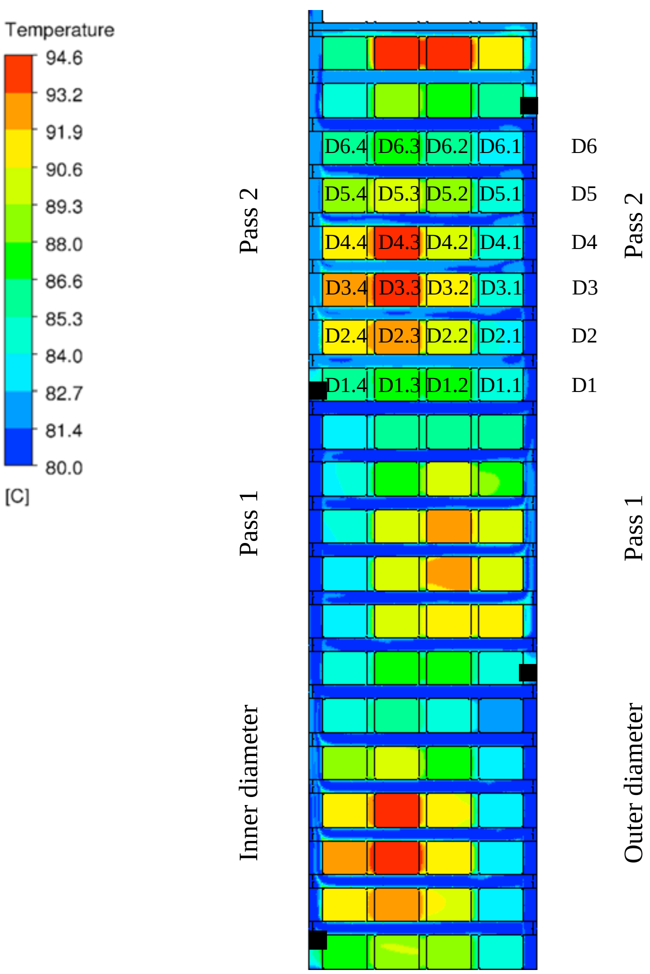

Fig. 14. Temperature distribution at $\dot{m}_{oil}$ = 9.0 kg/s, ϑ_{in} = 80°C and $P_{losses,i}$ = 360 W/turn.

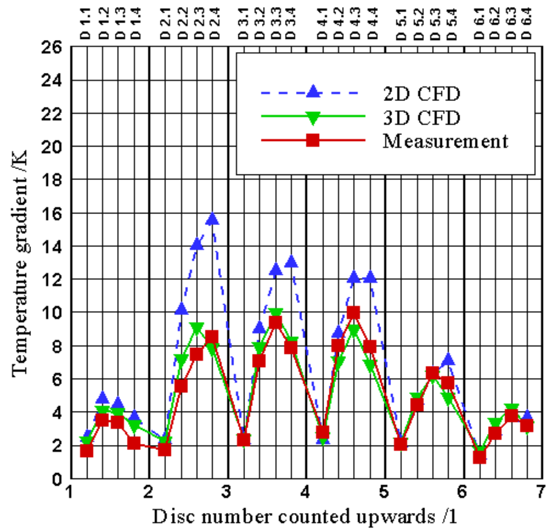

a) $\dot{m}_{oil}$ = 18.0 kg/s, ϑ_{in} = 80°C, pass 2

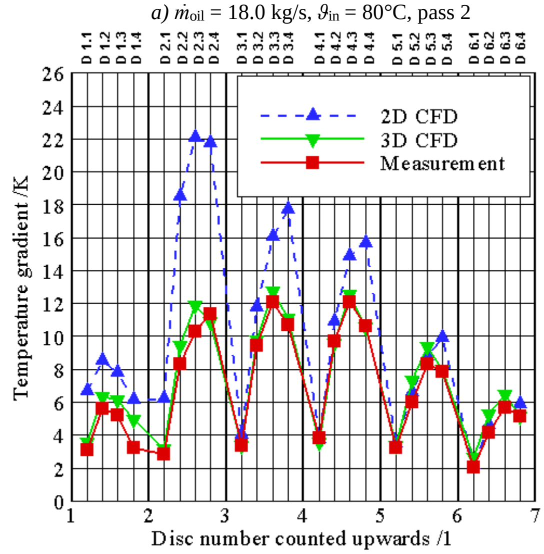

b) $\dot{m}_{oil}$ = 9.0 kg/s, ϑ_{in} = 80°C, pass 2

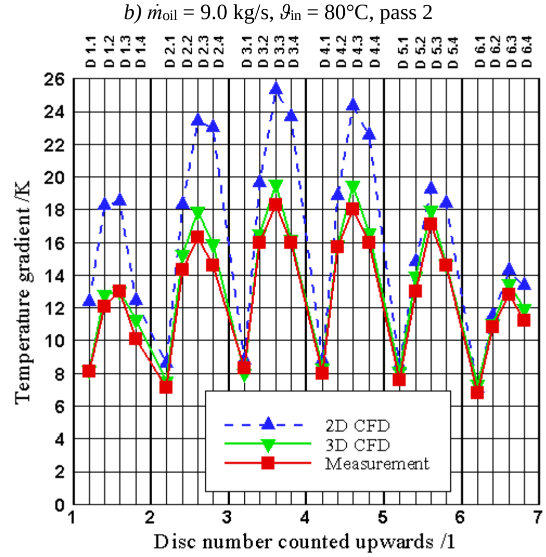

c) $\dot{m}_{oil}$ = 3.0 kg/s, ϑ_{in} = 80°C, pass 2

Fig. 15. Comparison of the measured temperature gradients with numerically determined 2D and 3D CFD results in pass 2 at various oil flow rates and with specific losses per winding turn of $P_{losses,\,i}$ = 360 W/turn.

This article has been accepted for publication in a future issue of this journal, but has not been fully edited. Content may change prior to final publication. Citation information: DOI 10.1109/TPWRD.2017.2711786, IEEE Transactions on Power Delivery

Next to the CFD results, the shown data also contains the measurements, allowing a proper assessment of the respective modelling approach. To calculate the local temperature gradient at a specific conductor, the oil temperature at the inlet of the pass holding that conductor is applied. In case of the measurements, oil temperatures are not measured but determined thermodynamically, taking the mass flow rate andthe specific thermal capacity of the oil together with all losses below the investigated pass into account.

The main advantage of the temperature gradients in comparison to absolute temperatures is the improved comparability of related results at different inlet temperatures. According to the 3D CFD results, a very good agreement with the experimental findings throughout the entire spectrum of investigated operating conditions can be observed. Deviations are in most of the cases below 1 K. Consequently, the 3D numerical modelling approach allows an accurate prediction of all relevant conductor temperatures at operating conditions that are representative for OD cooled disc windings. In addition, the application of 2D winding models might lead towards a conservative thermal design leaving room for a more cost effective winding layout.

VI. Conclusions

In this contribution, a 2D and 3D simulation model was presented to determine the oil speed of an OD cooled winding followed by an analysis of the hot-spot temperature and its position. The presented winding model, which has been validated by experimental results, provides useful insight into the horizontal cooling channels perpendicular to the main oil flow direction. The experimentally determined oil flow velocities and their optical investigation showed a good agreement with the corresponding numerical data and, thereby, confirmed the suitability of 3D numerical models to calculate the winding thermal behavior. The investigation indicated a strong non-uniform oil flow distribution on the horizontal channels influencing the position of the hot-spot. The study also showed that the oil flow velocity in the upper channels is greater than the lower ones. Correspondingly, the cooling in the lower channels is less and, therefore, the hot-spot occurs in the bottom area of each pass. The presented model can be utilized by transformer designers to optimize the cooling of power transformer windings.

References

[1] E. I. Amoiralis, M.A. Tsili and A.G. Kladas, “Transformer design and optimization: a literature survey,” *IEEE Transactions on Power Delivery*, vol. 24, no. 4, pp. 1999–2024, 2001.

[2] P. Picher, F. Torriano, M. Chaaban, and B. Girard, “Optimization of transformer overload using advanced thermal modelling,” *CIGRE 2010, Paris*, A2-305, 2010.

[3] J. Zhang, X. Li, “Oil cooling for disk-type transformer windings-part I: theory and model development,” *IEEE Transactions on Power Delivery*, Vol. 21, No. 3, 1318-1325, 2006.

[4] J. Zhang, X. Li, “Oil cooling for disk-type transformer windings-part II: parametric studies of design parameters,” *IEEE Transactions on Power Delivery*, Vol. 21, No. 3, 1326-1332, 2006.2006.

[5] Z. Radakovic, M. Sorgic, “Basics of detailed thermal-hydraulic model for thermal design of oil power transformers,” *IEEE Transactions Power Delivery*, Vol. 25, No. 2, 790-802, 2003.

[6] Z. Radakovic, K. Feser, “A new method for the calculation of the hotspot temperature in power transformers with ONAN cooling,” *IEEE Transactions on Power Delivery*, Vol. 18, No. 4, 1284-1292, 2003.

[7] H.M. R. Campelo, C. M. Fonte, R.C. Lopes, M.M. Dias and J. C.B. Lopes, “Network modelling applied to core power transformers and validation with cfd simulations,” *International Colloquium Transformer Research and Asset Management*, 2012.

[8] J. Codde, W. Van der Veken, and M. Baelmans, “Assessment of a hydraulic network model for zig-zag cooled power transformer windings,” *International Journal of Applied Thermal Engineering*, vol. 80, pp. 220-228, 2015.

[9] Transformer thermal modelling, *CIGRé Working Group*, A2.38, Tech. Rep., 2016.

[10] N. El Wakil, N.C. Chereches and J. Padet, “Numerical study of heat transfer and fluid flow in a power transformer,” *International Journal of Thermal Sciences*, Vol.45, pp.615-626. 2006.

[11] A. Skillen, *A. Revell, H. Lacovides and W. Wu*, “Numerical prediction of local hot-spot phenomena in transformer windings,” *International Journal of Applied Thermal Engineering*, vol. 36, pp. 96-105, 2012.

[12] J. Mufuta and E. Van, “Modeling of the mixed convection in the windings of a disc-type power transformer,” *International Journal of Applied Thermal Engineering*, vol. 20, pp. 417-437, 2000.

[13] J. Gastelurrutia, J.C. Ramos, G.S. Larraona, A. Rivas and J. Izagirre, “Numerical models of natural convection of distribution transformers,” International Journal of *Applied Thermal Engineering* Vol. 31, pp. 493-505, 2011.

[14] E.J. Kranenborg, C.O. Olsson, B.R. Samuelson, L/A. Lundin, and R.M. Missing, “Numerical study on mixed convection and thermal streaking in power transformer windings,” *Proc. of the 5th European Thermal-Sciences Conference*, The Netherlands, 2008.

[15] X. Zhang, Z. Wang and Q. Liu, “Prediction of pressure drop and flow distribution in disc type transformer winding in an OD cooling mode,” *IEEE Transactions on Power Delivery*, Vol. PP, No. 1, 2016, available online.

[16] F. Torriano, M. Chaaban and P. Picher, “Numerical study of parameters affecting the temperature distribution in a disc-type transformer winding,” *International Journal of Applied Thermal Engineering*, vol. 30, pp. 234-244, 2010.

[17] F. Torriano, P. Picher and M. Chaaban, “Numerical investigation of 3d flow and thermal effects in a disc-type transformer winding,” *International Journal of Applied Thermal Engineering*, vol. 40, pp. 121-131, 2012.

[18] Smolka, J. and A. J. Nowak, “Experimental validation of the coupled fluid flow, heat transfer and electromagnetic numerical model of the medium power dry-type electrical transformer,” *International Journal of Thermal Science*, vol. 47, no. 10, pp. 1393-1410, 2008.

[19] H. Campelo, M. Lopez- Fernandez, P. Picher and F. Torriano, “Advanced thermal modelling techniques in power transformers,” *Advanced Research Workshop on Transformers*, Spain, 2013.

[20] S. Tenbohlen, C. Breuer, F. Devaux, R. Lebreton, N. Schmidt, and T. Stirl, “Evaluation of the thermal performance of transformer windings by numerical investigations and measurements,” *CIGRE 2016, Paris*, A2-309, 2016.

[21] N. Schmidt, S. Tenbohlen, S. Chen, and C. Breuer, “Numerical and experimental investigation of the temperature distribution inside oil-cooled transformer windings,” *18th International Symposium on High Voltage Engineering*, ISH 2013, Seoul, South Korea, pp. 25.-30. Paper OG1-03, 2013.

[22] F. R. Menter, “Two-Equation Eddy-Viscosity Turbulence Models for Engineering Applications,” *AIAA Journal* vol. 32, no. 8, pp. 1598–1605, 1994.

[23] N. Schmidt: “Simulation and Experimental Validation of Forced Oil Flow in Power Transformers” (PhD thesis to be published in 2018 at the University of Stuttgart).

This article has been accepted for publication in a future issue of this journal, but has not been fully edited. Content may change prior to final publication. Citation information: DOI 10.1109/TPWRD.2017.2711786, IEEE Transactions on Power Delivery

BIOGRAPHIES

Stefan Tenbohlen (M'04, S'14) received his Diploma and Dr.-Ing. degrees from the Technical University of Aachen, Germany, in 1992 and 1997, respectively. 1997 he joined ALSTOM Schorch Transformatoren GmbH, Mönchengladbach, Germany, where he was responsible for basic research and product development. From 2002 to 2004 he was the head of the electrical and mechanical design department. 2004 he was appointed to a professorship and head of the institute of Power Transmission and High Voltage Technology of the University of Stuttgart, Germany. In this position his main research fields are high voltage technique, power transmission and electromagnetic compatibility (EMC). Prof. Tenbohlen holds several patents and published more than 400 papers. He is member of the IEEE, CIGRE SC A2 (Power Transformers), several international working groups and the chairman of German Power Engineering Society VDE-ETG FB Q2 (Materials, Electrical Insulations and Diagnostics).

Nicolas Schmidt received his Diploma degree in mechanical engineering from the University of Stuttgart in 2009. After his graduation, he joined the Institute of Power Transmission and High Voltage Technology at the University of Stuttgart. In 2015, he joined the Robert Bosch GmbH, Stuttgart, Germany, where he is responsible for thermal modelling of electronic control units.

Christian Breuer received his diploma degree in electrical engineering from the University of Applied Science – Georg Agricola. After his graduation in 2009, he joined GE Grid Solutions (former Areva and Alstom) as member of the research and development department. His main area of expertise is related to medium power transformers, e.g. creation of design rules and finite elements analysis.

Saeed Khandan received the M.Sc. degrees in heat transfer and fluid mechanical engineering in Iran, and is currently pursuing the Ph.D. degree in mechanical engineering. He has been a researcher and an assistant with the Institute of Power Transmission and High Voltage Technology, University of Stuttgart, Stuttgart, Germany since 2016. His principal research interest is in cooling system behaviors of power transformers.

Raphael Lebreton received his Ing. Diploma from the National Superior School of Electricity and Mechanics of Nancy France, in 2006. 2008 he joined Areva T&D where he was responsible for Partial Discharge monitoring research and development. Since 2014 he is also working on thermal optimization of transformers.